Root and Shoot Respiration of Perennial Ryegrass Are Supplied by the Same Substrate Pools: Assessment by Dynamic ^{13}C Labeling and Compartmental Analysis of Tracer Kinetics[1][OA]

Christoph Andreas Lehmeier, Fernando Alfredo Lattanzi*, Rudi Schäufele, Melanie Wild, and Hans Schnyder

Lehrstuhl für Grünlandlehre, Department für Pflanzenwissenschaften, Technische Universität München, D–85350 Freising-Weihenstephan, Germany

The substrate supply system for respiration of the shoot and root of perennial ryegrass (*Lolium perenne*) was characterized in terms of component pools and the pools' functional properties: size, half-life, and contribution to respiration of the root and shoot. These investigations were performed with perennial ryegrass growing in constant conditions with continuous light. Plants were labeled with $^{13}CO_2/^{12}CO_2$ for periods ranging from 1 to 600 h, followed by measurements of the rates and $^{13}C/^{12}C$ ratios of CO_2 respired by shoots and roots in the dark. Label appearance in roots was delayed by approximately 1 h relative to shoots; otherwise, the tracer time course was very similar in both organs. Compartmental analysis of respiratory tracer kinetics indicated that, in both organs, three pools supplied 95% of all respired carbon (a very slow pool whose kinetics could not be characterized provided the remaining 5%). The pools' half-lives and relative sizes were also nearly identical in shoot and root (half-life $<$ 15 min, approximately 3 h, and 33 h). An important role of short-term storage in supplying respiration was apparent in both organs: only 43% of respiration was supplied by current photosynthate (fixed carbon transferred directly to centers of respiration via the two fastest pools). The residence time of carbon in the respiratory supply system was practically the same in shoot and root. From this and other evidence, we argue that both organs were supplied by the same pools and that the residence time was controlled by the shoot via current photosynthate and storage deposition/mobilization fluxes.

This article deals with the substrate supply system of respiration in roots and shoots of intact plants of perennial ryegrass (*Lolium perenne*). This system is an integral part of the total pool of available substrates for growth and maintenance processes in the root and shoot and a major sink for carbon fixed in photosynthesis (Amthor, 1989). In the narrow sense, respired carbon mainly derives from a few compounds: malate, pyruvate, isocitrate, α-ketoglutarate, or gluconate-6-P (Heldt, 2005), which together account for only a small fraction of total plant biomass. Conversely, in the broad sense, all respired carbon derives from photosynthesis, and, ultimately, most of the carbon fixed in photosynthesis is returned back to the atmosphere by way of respiration (Schimel, 1995; Trumbore, 2006). Before being respired, carbon may visit various biochemical compounds in different organs. In principle, the physical and biochemical paths taken by carbon before being used as a substrate in respiration can be intricate, reflecting the physical and biochemical complexity of plant metabolic networks (ap Rees, 1980; Plaxton and Podestá, 2006).

The intermediary fate (or allocation history) of carbon controls its residence time inside the plant (i.e. the lapse of time between fixation and respiration). Thus, for instance, if carbon fixed in photosynthesis is transferred directly to centers of respiration, then the residence time in the plant is short (seconds to minutes). In contrast, if carbon is first deposited in long-lived molecules (such as proteins or storage carbohydrates), then the residence time is long (days to months). Respired carbon, therefore, originates from a heterogeneous mixture of molecules that cycle more or less extensively through a network of biochemical compounds and physical compartments. So the residence time of respired carbon reveals functional properties of the supply system feeding respiration and can be used to shed light on structural-functional differences between supply systems feeding different plant parts, such as roots and shoots. We are not aware of any comparative studies of the residence time of carbon feeding shoot and root respiration.

The residence time of carbon can be characterized by quantitative tracer techniques (Ryle et al., 1976; Kouchi et al., 1985; Schnyder et al., 2003; Lötscher and

[1] This work was supported by the Deutsche Forschungsgemeinschaft (SFB 607).

* Corresponding author; e-mail lattanzi@wzw.tum.de.

The author responsible for distribution of materials integral to the findings presented in this article in accordance with the policy described in the Instructions for Authors (www.plantphysiol.org) is: Fernando Alfredo Lattanzi (lattanzi@wzw.tum.de).

[OA] Open Access articles can be viewed online without a subscription.

www.plantphysiol.org/cgi/doi/10.1104/pp.108.127324

Gayler, 2005). Studies at the level of whole plants (Schnyder et al., 2003) or with root systems (Kouchi et al., 1985, 1986; Lötscher and Gayler, 2005) have revealed two distinct phases in the kinetics of tracer appearance in respired CO_2: a phase with fast label appearance, which indicated a supply component that was closely connected with current photosynthetic activity; and a phase with slow label appearance, which indicated the participation of one (or more) store(s) in supplying respiration. Several types of compounds, including starch, vacuolar Suc, and fructan, as well as proteins have been suggested as stores supplying substrates for respiration (ap Rees, 1980; Farrar, 1980). It is unknown if the contribution of stores and products of current assimilation to respiration is the same or different in shoots and roots.

Whereas most of the interpretations of label appearance (in dynamic labeling), or label disappearance (in pulse-chase labeling), in respired CO_2 have been qualitative, the tracer kinetics can also be quantitatively and mechanistically interpreted in terms of the number, size, kinetic properties (half-life, turnover rate), and contribution of the pools that constitute the supply system of respiration. This is best done using the mathematical methodology of compartmental analysis (Atkins, 1969; Jacquez, 1996), which has been applied to various problems of the assimilation, transport, and metabolism of carbon in plants (Moorby and Jarman, 1975; Prosser and Farrar, 1981; Rocher and Prioul, 1987; Bürkle et al., 1998; Lattanzi et al., 2005). A pool is defined here as a set of compounds that exhibit the same proportion of labeled carbon atoms; that is, a pool represents a "space" in which the isotopic composition is uniform (Rescigno, 2001). So, in principle, one pool can include several populations of anatomical (physical) features and biochemical species on the condition that they exhibit the same proportion of label. Most importantly, however, by characterizing the pool on the basis of respiratory tracer release, the pool is identified by its function: supplying respiration with substrate.

Here, we use compartmental analysis to provide a quantitative description and comparison of the compartmental structure and kinetic properties of the supply system feeding root and shoot respiration. Specifically, we address the following questions: What are the kinetics and sizes of the major respiratory pools supplying carbon to respiration of ryegrass? How are these pools connected? How do shoot and root differ in terms of carbon supply by those pools? And what are the contributions of current assimilation and stores to respiration?

One basic difficulty in the characterization of carbon pools supplying respiration is a sufficient range of tracer application (or chase) times. Putative substrates for respiration have turnover times in the range of less than 1 h to many days (Simpson et al., 1981; Dungey and Davies, 1982; Farrar and Farrar, 1986; Rocher and Prioul, 1987; Schnyder et al., 2003) or possibly weeks, meaning that labeling (or chase) times must vary by about 4 orders of magnitude if all components of the respiratory supply system are to be characterized. Typically, however, the range of tracer exposure (or chase) times has been much narrower, thus capturing only fast or slow pools. In this study, we aimed to characterize all major components of the respiratory supply system by using labeling times ranging from 1 to 600 h. To this end, we labeled all carbon assimilated by individual plants with a known constant $^{13}C/^{12}C$ ratio in CO_2 over a period of up to 25 d, when respired CO_2 had reached 95% label saturation (this labeling method is termed "steady-state labeling" in "classical" plant physiology literature [Geiger and Swanson, 1965; Geiger et al., 1969] but is now referred to as "dynamic labeling" [Ratcliffe and Shachar-Hill, 2006]). The $^{13}C/^{12}C$ ratio of respiratory CO_2 produced in the root and shoot was measured at various times, and the time course of tracer in respired CO_2 was evaluated with compartmental analysis.

RESULTS

Meeting the Steady-State Conditions of Compartmental Analysis: Constant Specific Growth and Respiration Rates

Inferring the number and kinetics of mixing pools by compartmental analysis relies on several assumptions (presented in full, and their validity discussed, in "Materials and Methods"). A major one is that the system under consideration shows no change in time except for tracer content (referred to as "metabolic steady state" by Ratcliffe and Shachar-Hill, 2006). By performing this study in controlled environments, constant growth conditions were provided: plants grew with continuous illumination, and temperature, relative humidity, and CO_2 concentration were maintained at constant values throughout the experiment. Water and nutrients were supplied frequently.

During the experiment, shoots and roots exhibited constant specific growth rates (shoot, 0.085 g carbon [C] g^{-1} shoot C $d^{-1} \pm 0.011$, $CI_{0.95}$; root, 0.072 g C g^{-1} root C $d^{-1} \pm 0.014$, $CI_{0.95}$). Moreover, specific respiration rates were steady throughout the labeling period ($P > 0.05$; Fig. 1), with shoot respiration (0.97 mg C g^{-1} plant C $h^{-1} \pm 0.13$ SD; $n = 60$) being nearly twice as high as root respiration (0.53 mg C g^{-1} plant C $h^{-1} \pm 0.09$ SD; $n = 60$). Furthermore, due to the similarity of shoot- and root-specific growth rates, the shoot to root ratio (3.8 g C g^{-1} C) was nearly constant. No differences in the rates of growth and respiration were observed between growth chambers ($P > 0.05$). These results indicate that plants were growing nearly exponentially, with constant specific demands on respiration; thus, the system was virtually in a steady state.

Water-Soluble Carbohydrate Concentration in Root and Shoot Biomass

Water-soluble carbohydrates accounted for 0.337 g C g^{-1} total shoot C (± 0.035 SD; $n = 6$). This was more

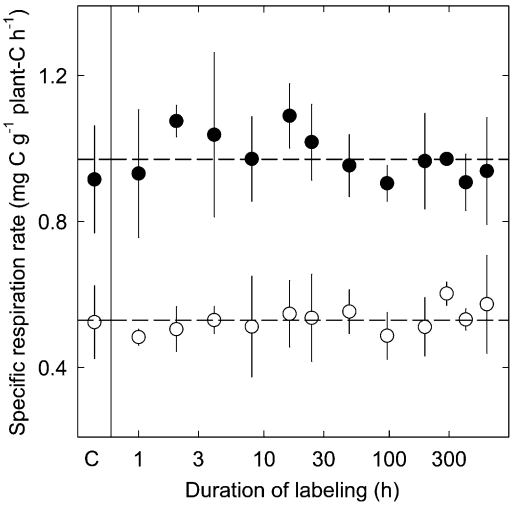

Figure 1. Specific respiration rates of shoots (black symbols) and roots (white symbols) of perennial ryegrass, labeled for different time intervals, and of nonlabeled controls (C; at left). Each value is the mean of four to 10 replicate plants (±SD). Dashed lines indicate average values (see "Results"). Note the logarithmic scaling of the *x* axis.

than four times higher than the concentration in the roots (0.079 g C g^{-1} root C ± 0.006 SD; $n = 6$).

Labeling Kinetics of Respired CO_2 in the Shoot and Root

The time courses of tracer incorporation into shoot- and root-respired CO_2 were strikingly similar (Fig. 2), except that first label incorporation into respiratory CO_2 of roots occurred with a delay of approximately 1 h and that the degree of labeling of root-respired CO_2 was about 5% less than that of shoots during the first week of labeling.

The labeling kinetics revealed five distinct phases: (1) a fast initial labeling; (2) a lag period of a few hours, in which the degree of labeling did not change (Fig. 2, insets); (3) a period that lasted until about 1 d of labeling, in which the fraction of unlabeled carbon decreased rapidly; (4) a period until about 8 d, in which the fraction of unlabeled carbon decreased at a slower rate; and (5) a final period that lasted until the end of the experiment (25 d of labeling), in which the fraction of unlabeled carbon in respiration remained near 5% (Fig. 2).

Compartmental Model of Substrate Pools for Respiration

The labeling kinetics reflected the operation of a substrate pool system supplying respiration. The structure of this system (number of pools, links between pools, delays, and sites of tracer entry and outlet) was determined by analysis of the tracer kinetics of respiratory CO_2 (Fig. 2), including multiexponential curve fitting to the tracer kinetics (similar to that described by Moorby and Jarman, 1975) and consideration of established compartmental concepts of respiratory carbon metabolism (Farrar, 1990; Dewar et al., 1998) while respecting the (reductionist) principle of parsimony ("all other things being equal, the simplest solution is the best"). (1) The fast initial labeling of respired CO_2 (phase 1) revealed a respiratory activity fed by a substrate pool very close to photosynthetic metabolism and hence rapidly renewed by assimilated tracer. This pool was named Q_1, and its respiratory activity was named F_{10}. (2) Further respiratory tracer release occurred only after a delay of several hours (phase 2), revealing the existence of a second respiratory activity (F_{20}) fed via another pool. (3) Fitting of a dual-exponential (instead of a monoexponential) decay function to the tracer kinetics beyond 4 h of labeling increased the goodness of fit and gave a better distribution of residuals. More exponential terms, however, improved neither the fit nor the distribution of residuals. This indicated the existence of (at least) two additional respiratory substrate pools with distinct turnover times (phases 3 and 4). These pools were named Q_2 and Q_3. (4) A small residual respiratory activity (approximately 5%; phase 5) could not be characterized in terms of pool size and half-life because it released no tracer during the duration of

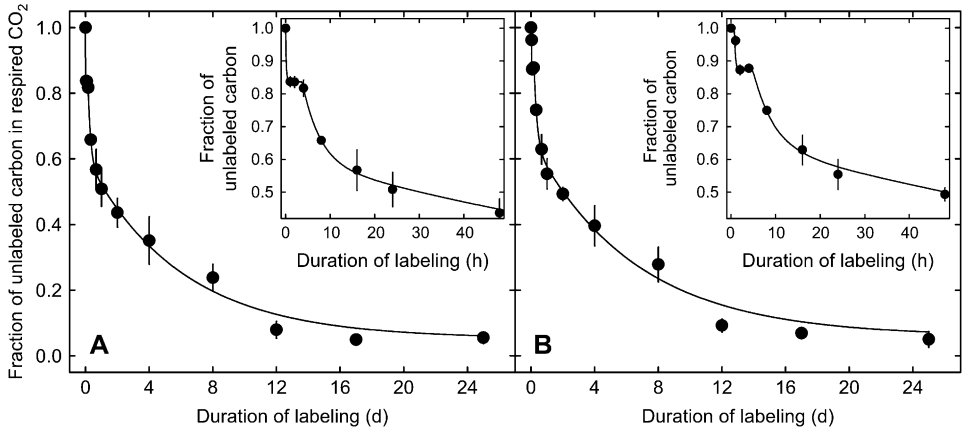

Figure 2. Evolution of the fraction of unlabeled carbon ($f_{unlabeled}$) in CO_2 respired by shoots (A) and roots (B) of perennial ryegrass during labeling. Each value is the mean of four to six replicate plants (±SE). Lines denote model predictions (Fig. 3). Insets expand the first 48 h.

labeling. (5) The fact that pools Q_2 and Q_3 were resolved by respiratory tracer kinetics meant that respiratory activity F_{20} was fed via Q_2, the faster of the two pools. (6) Of the several possibilities to arrange pool Q_3 in the model (e.g. by exchanging with Q_1, Q_2, or with both Q_1 and Q_2), we chose the simplest and biologically most meaningful: pool Q_3 supplied respiration by acting as a store, thus, by exchanging carbon with Q_2. (7) The 0.8-h delay in labeling of respiratory CO_2 in roots relative to that in the shoot was interpreted as the time required for phloem transport of tracer from shoot to root.

A three-pool model with one delay was capable of accounting for all of the above-mentioned features of shoot respiration (delay 1 in Fig. 3). The same model with an additional (approximately 0.8 h) delay for tracer release fitted root respiration (delay 2). In this model, a map of respiratory carbon metabolism of the shoot and the root, carbon fixed in photosynthesis entered the respiratory system via Q_1, where it was either respired or transferred to Q_2. In Q_2, carbon was either respired directly or first cycled through Q_3 before being respired via Q_2. This is not the simplest three-pool model (that would consist of three independent and isolated pools, each receiving tracer and each releasing CO_2), but it is the simplest with biological consistency able to reproduce the observed tracer kinetics. Additional pools were not supported by the number of exponential terms found, and different arrangements of pools and fluxes were not supported by goodness of fits (e.g. linking Q_3 to Q_1 instead of to Q_2).

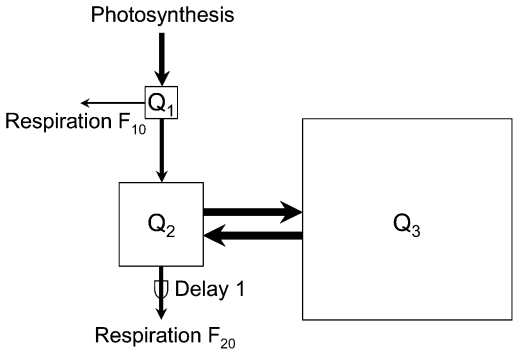

Figure 3. Three-pool model of the substrate supply system of dark respiration of the shoot of perennial ryegrass. Carbon fixed in photosynthesis enters the respiratory system via pool Q_1, where it is either respired (respiratory flux F_{10}) or transferred to pool Q_2. In Q_2, carbon is either respired directly (F_{20}) or first cycles through Q_3 before being respired via Q_2. Respiratory tracer release from Q_2 is associated with a delay. Functional characteristics of the pools (size, half-life, and contribution to shoot and root respiration; Table I) were estimated by translating the model into a set of differential equations and fitting the model to the tracer kinetics of shoot respiration. The same model also fitted the tracer kinetics of dark respiration of the root but included an additional delay of 0.8 h for tracer release in F_{10} and F_{20}. Arrows and boxes are scaled to indicate the magnitude of fluxes and pool sizes.

This model was translated into a set of differential equations (similar to Lattanzi et al., 2005), which described the system in terms of fluxes between pools and the environment, and implemented in a custom-made program using the free software R (R Development Core Team, 2007). This program systematically tested millions of preset values for pool sizes, fluxes between pools, and delays to find the lowest root mean squared error (RMSE). This extensive evaluation (1) ensured that the absolute minimum RMSE was identified rather than a "local" minimum, and (2) revealed its sensitivity to changes in parameter values (Fig. 4). These procedures were performed independently for the shoot and root data, thus generating independent estimates of system properties for the shoot and root.

Pool Sizes, Half-Lives, and Contributions to Respiration

Pool half-lives were derived from fitted pool sizes and fluxes. The contribution of each pool to respiration was determined as the probability of carbon cycling through that pool before being respired. Pools Q_1, Q_2, and Q_3 differed greatly in size and half-life (Table I). The relative sizes of the three pools were similar in the shoot and root, but root pools were 30% to 50% smaller than shoot pools, because root respiration rate was half that of the shoot (Fig. 1).

Q_1 was a very small, rapidly turned-over pool. Both in the shoot and in the root, it was equivalent to 0.02% of total plant carbon, and its half-life was on the order of 0.1 to 0.2 h. Q_2 of the shoot represented approximately 1% and Q_2 of the root represented approximately 0.7% of total plant carbon, and both had half-lives of approximately 3 h (Table I). Q_3 was the largest: its shoot component constituted 7% and the root component constituted 4.5% of total plant carbon. The half-life of Q_3 was virtually identical in both organs: 33 h. In total, 13.2% of all plant carbon formed part of respiratory substrate pools.

Although Q_1 was a very small pool, it served a significant role in respiration: 16% of shoot-respired carbon and 13% of root-respired carbon cycled only through Q_1 (Table I). The bulk, 79% of shoot respiration and 82% of root respiration, was supplied by Q_2. Respiration via Q_2 was supplied by direct transfer of current photosynthate via Q_1 and by carbon that first cycled through Q_3 (Fig. 3). Direct transfer accounted for 28% of shoot respiration and 27% of root respiration. This meant that two pools whose carbon was renewed very rapidly by current photosynthetic assimilation supplied 44% of shoot respiration and 40% of root respiration. On the contrary, Q_3, with a half-life of 33 h, played a (short-term) storage role and was the main source of substrates for respiration: 51% of all carbon respired in the shoot and 55% of that respired in the root cycled through this pool at least once before being respired (Table I). In both organs, 5% of respired carbon derived from a pool that could not be characterized in terms of size and half-life. Sensitivity analyses showed that estimates of pool size, half-life, and

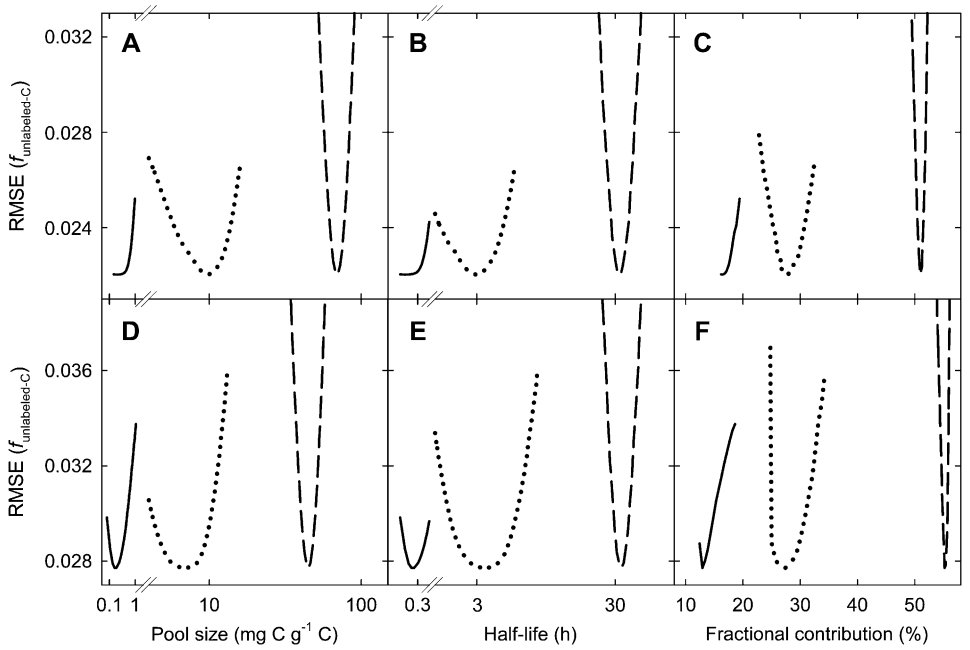

Figure 4. Sensitivity of the goodness of model fits for the shoot (A–C) and the root (D–F) to departures from optimized values of pool size (A and D), half-life (B and E), and contribution to respiration (C and F). Sensitivity is expressed by the RMSE of the fit (minimum RMSE indicates the optimum value of a model parameter). The solid lines represent Q_1, the dotted lines represent Q_2, and the dashed lines represent Q_3. Note the logarithmic scaling of the *x* axis for pool size and half-life.

contributions to respiration were well constrained by the data (Fig. 4).

DISCUSSION

The Identity of Respiratory Substrate Pools

This work indicates the existence of three pools supplying 95% of all substrate for respiration in intact plants of perennial ryegrass. A most distinctive difference between these pools was the speed of carbon exchange by current assimilate: half-lives differed by almost 4 orders of magnitude between the fastest (Q_1) and the slowest (Q_3) pool (Table I; Fig. 4). Each of these pools likely did not represent a single biochemical compound with a specific spatial location; rather, they were probably mixtures of substrates distributed in different tissues and organs throughout the plant. Heterogeneous as they may be, these mixtures nonetheless shared a common pattern of tracer incorporation/release that compartmental analysis recognized. Hence, derived half-lives can be compared with known half-lives of putative substrates for respiration with the aim of attributing functional-biochemical identities to Q_1, Q_2, and Q_3.

Q_1 very quickly incorporated and released tracer. Thus, it was intimately connected with both CO_2 fixation and respiration. Its rapid turnover rate is consistent with the speed of labeling of primary photosynthetic products that are also involved in decarboxylation, including organic acids (Calvin and Bassham, 1962). Q_1 also contributed to root respiration, indicating a phloem-translocated component. Malate could have been a major constituent of Q_1: it is rapidly labeled in leaves (Heber and Willenbrink, 1964), it is translocated to roots (Imsande and Touraine, 1994), and it is thought to be decarboxylated there (Imsande and Touraine, 1994; Stitt et al., 2002). Malate concentration is high in plants growing on nitrate (Leport et al., 1996) and may serve as a control and substrate for the nitrate uptake system (Imsande and Touraine, 1994). If this conclusion is true, then the relevance of Q_1 would depend on nitrogen source. We know of no other comparative studies of whole shoot and root respiratory tracer kinetics that would allow an assessment of the generality of our

Table I. *Optimization results for the parameters of the model shown in Figure 3, as applied to the tracer time courses of shoot and root respiration (Fig. 2)*

Model parameters include the size, half-life, and percentage contribution to respiration of pools Q_1, Q_2, and Q_3. Together, the three pools accounted for 95% of shoot and root respiration. The remainder was supplied by sources that released no tracer within the 25-d-long labeling period (Fig. 2). The quality of the fits is expressed as the RMSE.

Pool	Shoot	Root
	size (mg C g^{-1} plant C)	
Q_1	≤0.2	≤0.2
Q_2	9.7	6.9
Q_3	70.3	45.0
	half-life (h)	
Q_1	≤0.1	≤0.2
Q_2	2.9	3.4
Q_3	33.0	33.2
	contribution (%)	
Q_1	16	13
Q_2	28	27
Q_3	51	55
	delay 1 (h)	
–	3.7	4.1
	delay 2 (h)	
–	–	0.8
	RMSE	
–	0.022	0.028

findings. Nogués et al. (2004) reported a rapid incorporation of tracer in CO_2 respired by *Phaseolus vulgaris* leaves, consistent with tracer kinetics in Q_1. But no study of tracer incorporation in root respiration has reported the existence of Q_1. Perhaps the participation of Q_1 in respiration is not a ubiquitous feature. An essential factor in identifying Q_1 was the existence of a lag of a few hours between tracer incorporation and release from Q_2 (see below). Had there been no lag, then tracer release from Q_2 would have overlain that of Q_1, rendering it unnoticeable.

The half-life of Q_2 (3 h) was close to, but longer than, the half-life often ascribed to a pool of "transport Suc" (1–2 h; Moorby and Jarman, 1975; Bell and Incoll, 1982; Farrar and Farrar, 1986). This pool is composed of Suc in the cytoplasm, apoplast, and sieve tubes and companion cells of the phloem in actively photosynthesizing and exporting C3 leaves (Geiger et al., 1983). Our study derived respiratory pool kinetics from measurements at the scale of whole shoots and roots; that is, from tissues of very different developmental status: growing (sink), mature, and senescing. We know of no studies of the kinetics of the transport pool in vegetative sink tissues. In the leaf growth zone of *Festuca arundinacea*, the turnover rate of total tissue Suc varied between less than 1 h and approximately 4 h, depending mainly on growth rate and related Suc import and use (Schnyder and Nelson, 1987). Suc turnover in metabolically active sink tissue, it seems, would be similar to that in actively photosynthesizing leaves. Therefore, an interpretation of the half-life of 3 h of Q_2 is that it represents the (activity-weighted) mean of the kinetics of the transport pool extending over both source and sink tissues in the plant.

There was a substantial delay between tracer uptake and respiratory tracer release from Q_2 (delay 1; Figs. 2 and 3; Table I). This effect was observed in both shoot and root; therefore, it must have been related to metabolism and not to transport. Results of others suggest some delay between the arrival of Suc in sink tissue and its use in respiration: in a study with *F. arundinacea*, Allard and Nelson (1991) found that 90% of the tracer imported into leaf growth zones was still present in the water-soluble carbohydrate fraction at 2 h after labeling source leaves, and hardly any label was present in structural material. In the work of Kouchi et al. (1985) and Lötscher and Gayler (2005), respiratory tracer release from roots of legumes did not start until approximately 2 h or longer after the beginning of labeling. But Dilkes et al. (2004) observed a very rapid labeling of root exudates in wheat (*Triticum aestivum*) and no evidence for a marked delay between tracer release via exudates and respiration. A similar lag was observed in other experiments with perennial ryegrass growing with a limited supply of nitrogen (C.A. Lehmeier, F.A. Lattanzi, R. Schäufele, and H. Schnyder, unpublished data), showing that our observation was not a singular result. We cannot rule out the possibility that growth in continuous light was a factor. However, we cannot envisage the physiological mechanism of such an effect.

The half-life of 33 h and the large size of Q_3 suggest a storage pool. Nonstructural carbohydrates are generally considered as the main source of respired carbon (ap Rees, 1980; Tcherkez et al., 2003), and some of them are used as temporary stores (Smith and Stitt, 2007). In C_3 grasses, such as perennial ryegrass, carbohydrate storage occurs mainly in vacuoles in the form of Suc or fructan (Farrar and Farrar, 1986; Pollock and Cairns, 1991; Vijn and Smeekens, 1999). Starch was only a trace component of biomass in this study (<1% of plant dry weight; data not shown), but water-soluble carbohydrates were present at high concentration, particularly in the shoot. A storage pool with a half-life in the range of 12 to 24 h is often found in C3 plants and ascribed to vacuolar Suc (Moorby and Jarman, 1975; Bell and Incoll, 1982; Farrar and Farrar, 1986). The dynamics of fructan turnover are less clear. Its half-life was found to be in the range of 2 to 5 h in leaf blades of *Hordeum distichum* and two *Poa* species (Borland and Farrar, 1988; Farrar, 1989) and 14 to 18 h in leaf sheaths of *Poa* (similar to a 9- to 15-h half-life of vacuolar Suc; Borland and Farrar, 1988). Fructan stored in wheat stems did not turn over during the storage phase (Winzeler et al., 1990).

Proteins constitute another large plant fraction in which turnover is closely connected with respiratory pathways (Lea and Ireland, 1999). Half-lives of soluble proteins are on the order of 3.5 to 8 d (Simpson et al., 1981; Dungey and Davies, 1982), much longer than the half-life of Q_3. This indicates that if proteins contributed to Q_3, then this contribution must have been relatively small. Forcing the model to split Q_3 into two storage pools gave tentative support to this conclusion, as it yielded one pool with a half-life of 20 h contributing approximately 40% of total respiration and the other pool with a half-life of approximately 4 d contributing approximately 10% of total respiration.

The Size of the Respiratory Substrate Pool System and Carbon Use Efficiency

Collectively, the respiratory substrate pool system constituted 13.2% of the total carbon mass of plants, and most of this (approximately 87%) was contained in Q_3, the storage pool. In comparison, water-soluble carbohydrates accounted for 28% of total plant carbon, meaning that it contained much more carbon than all respiratory pools combined. This is expected because stores supply not only respiration but also carbon skeletons for new biomass. Assuming that water-soluble carbohydrates were the exclusive substrate for respiration (thus neglecting any contribution of other putative substrates, such as malate or proteins), then 47% of the water-soluble carbohydrate carbon was allocated to respiratory CO_2. In that case, the remainder (53%) must have been allocated to new (structural) biomass. This corresponds to a carbon use efficiency (CUE) of 53% for water-soluble carbohydrates. This is a conservative (i.e. low) estimate of the CUE of water-soluble carbohydrates, as it ignores possible contributions to

respiration by other substrates. Yet, this efficiency is close to empirical and theoretical estimates of photosynthetic CUE in young herbaceous plants (van Iersel, 2003).

Are Shoot and Root Respiration Supplied by the Same Pools?

The most striking result of this work was the great similarity of root and shoot respiratory tracer kinetics. This meant that the same compartmental model fitted the root and shoot data equally well (Table I; Figs. 2 and 4): number of pools, their half-lives and relative sizes, and their relative contributions to respired carbon were practically the same in both organs. The only notable difference was that tracer appearance in root respiration was delayed by approximately 0.8 h (delay 2; Table I), a time entirely in agreement with phloem transport velocity (Windt et al., 2006). These features are consistent with a single three-pool system feeding shoot and root respiration.

If the supply system for root and shoot respiration consisted of only three pools, where were they located? Q_1 and Q_2 supplied respiration directly and were active in the root and shoot (Fig. 3), so both must have had shoot and root compartments connected via the phloem. Conversely, a large part of Q_3 must have been located in the shoot. This is because the "root component" of Q_3 would have been equivalent to greater than 30% of the carbon mass of the root system (calculated by multiplying Q_3 root of 45 mg C g^{-1} plant C with the shoot to root ratio of 3.8 and dividing by the estimated CUE of 0.53), a value much greater than the total mass of nonstructural carbon in the roots (water-soluble carbohydrates, 7.9% of root carbon; protein, 10% of root carbon, estimated from nitrogen content and a 3.1 carbon to nitrogen ratio). So, only a fraction of the respiratory CO_2 of roots could have come from stores located in the root. Accordingly, most of the Q_3-derived respiratory CO_2 of roots must have come from the shoot store(s). Indeed, as is typical in grasses (Sullivan and Sprague, 1943; Davidson and Milthorpe, 1966a), the bulk of nonstructural carbohydrates and protein (94% and 83% of plant total, respectively) were contained in the shoot.

The Role of Stores and Current Photosynthesis in Supplying Respiration

More than half of respired carbon cycled, at least once, through a storage pool before being respired. Clearly, stores were a central part of respiratory carbon metabolism. That a significant fraction of respiration is supplied by stores has been suggested before (Kouchi et al., 1985, 1986; Dilkes et al., 2004; Lötscher and Gayler, 2005), although the kinetic properties of pools were not determined in these studies, nor were the localization and operating controls discussed. This study revealed that these carbon stores were quite short lived and, therefore, might have a limited capacity to sustain current carbon use rates over extended periods.

Yet, carbon stores used in respiration showed a longer half-life (this study) than those supplying leaf growth (Lattanzi et al., 2005). Thus, leaf growth seems to be much more dependent on continued assimilation of carbon, which agrees well with results on carbon allocation shortly after severe defoliation: most carbon used for leaf growth was new (Avice et al., 1996; Schnyder and de Visser, 1999), while that sustaining root respiration was largely old (Avice et al., 1996). Indeed, rapid and drastic decrease of root respiration following defoliation (Davidson and Milthorpe, 1966b) may be due to the fact that substrate for root respiration is essentially derived from current CO_2 fixation and stores in the shoot. Thus, the localization of most of the respiratory substrate in the shoot indicates that the control of root activity by the shoot would occur via the control of both current photosynthate and storage mobilization.

In conclusion, this work revealed a tight plant-level integration of respiratory substrate pools and fluxes. Incidentally, the results of this work suggest that the tracer kinetics of root respiration can be inferred from that of the shoot (which was nearly identical to that of the root), which is useful information for partitioning of autotrophic and heterotrophic respiration in ecosystem-scale studies. Future work should address the possible variability and controls of substrate pool properties (half-life and size) and their contributions to root and shoot respiration.

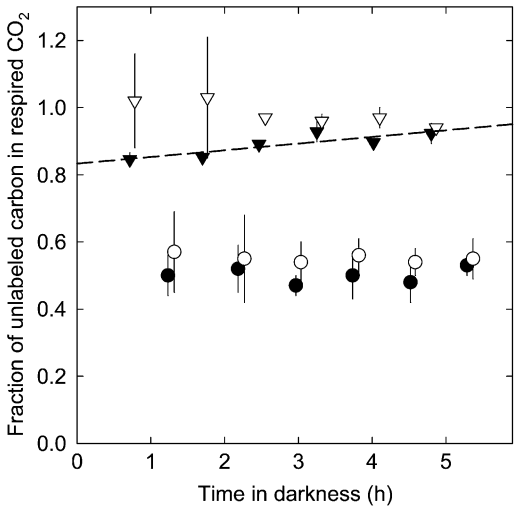

Figure 5. Time course of the fraction of unlabeled carbon in CO_2, respired by shoots (black symbols) and roots (white symbols) of perennial ryegrass plants during respiration measurements, for plants that were previously labeled for 1 h (triangles) and 24 h (circles). Error bars denote SE ($n = 4$). The dashed line denotes the linear regression for shoots labeled for 1 h ($y = 0.83 + 0.48\ x$, $r^2 = 0.74$; see "Materials and Methods"). The regression for the other labeling times was nonsignificant (data not shown).

MATERIALS AND METHODS

Plant Material and Growth Conditions

Seeds of perennial ryegrass (*Lolium perenne* 'Acento') were sown individually in plastic pots (350 mm height, 50 mm diameter) filled with 800 g of washed quartz sand (0.3–0.8 mm grain size). The bottom of every pot had a drainage hole (7 mm diameter) covered with a fine nylon net. Pots were arranged in plastic containers (760 × 560 × 320 mm) at a density of 378 plants m^{-2}. Two containers were placed in each of two growth chambers (Conviron E15; Conviron). Plants were grown in continuous light supplied by cool-white fluorescent tubes. Irradiance was maintained at 275 mol m^{-2} s^{-1} photosynthetic photon flux density at the top of the canopy. Temperature was controlled at 20°C, and relative humidity was kept near 85%. The stands were irrigated by flooding the boxes every 3 h briefly with modified Hoagland solution [2.5 mM $Ca(NO_3)_2$, 2.5 mM KNO_3, 1.0 mM $MgSO_4$, 0.18 mM KH_2PO_4, 0.21 mM K_2HPO_4, 0.5 mM NaCl, 0.4 mM KCl, 0.4 mM $CaCl_2$, 0.125 mM iron as EDTA, and micronutrients). Stands were periodically flushed with demineralized water to prevent salt accumulation.

CO_2 Control in the Growth Chambers

The two growth chambers formed part of the $^{13}CO_2/^{12}CO_2$ gas exchange and labeling system described by Schnyder et al. (2003). Air supply to the chambers was performed by mixing CO_2-free air and CO_2 with known carbon isotope composition ($\delta^{13}C$, with $\delta^{13}C = [(^{13}C/^{12}C_{sample})/(^{13}C/^{12}C_{international\ VPDB\ standard})] - 1$) using mass flow controllers. Control was facilitated by measuring concentration and $\delta^{13}C$ of CO_2 online every 20 to 30 min by an infrared gas analyzer (IRGA; Li-6262; Li-Cor) and a continuous-flow isotope-ratio mass spectrometer (CF-IRMS; Delta Plus; Finnigan).

One chamber received ^{13}C-depleted CO_2 ($\delta^{13}C$, −28.8‰), and the other received ^{13}C-enriched CO_2 ($\delta^{13}C$, −1.7‰; both from Linde AG). The $\delta^{13}C$ and concentration of CO_2 (360 μL L^{-1}) inside the chambers were kept nearly constant by periodically adjusting air flow and CO_2 concentration in the inlet air of each chamber. The rate of CO_2 supply to the chambers exceeded the CO_2 exchange rate of the plant stands by a factor of 9. This minimized the effects of photosynthesis and respiration on $\delta^{13}C$ and the concentration of CO_2 in the chambers and suppressed the recycling of respiratory CO_2.

Chamber doors were equipped with custom-made transparent air locks that had small ports through which plants could be handled and sampled. These air locks ensured minimal disturbance of the $\delta^{13}C$ and concentration of CO_2 in the chamber atmosphere when chambers had to be opened during the experiment. Empty chamber tests of air locks demonstrated that with doors opened for 20 min, the CO_2 concentration in the chambers changed by only 4 μL L^{-1} and $\delta^{13}C$ changed by about 1‰. Twenty minutes after closing the chambers, CO_2 concentration and $\delta^{13}C$ in the chambers had returned to set-point values.

^{13}C Labeling

From 3 weeks after imbibition of seeds, when plants had three tillers, individual plants were labeled by swapping randomly selected plants between chambers. Thus, plants growing in the chamber with ^{13}C-enriched CO_2 were transferred to the chamber with ^{13}C-depleted CO_2, and vice versa. Plants were kept in the presence of the "new" CO_2 for 1, 2, 4, 8, or 16 h or for 1, 2, 4, 8, 12, 17, or 25 d. At the end of the given labeling intervals, plants were removed from the stands and transferred to a root/shoot respiration measurement system. This was done for at least four replicate plants for each labeling interval. To minimize possible size- and development-related effects on respiration, labeling periods were scheduled in such a way that labeling duration and plant age at sampling were not correlated.

Respiration Measurements

Shoot and root respiration rates as well as the $\delta^{13}C$ of shoot- and root-respired CO_2 of individual plants were measured in the gas-exchange system described and used by Lötscher et al. (2004) and Klumpp et al. (2005). This system included four single-plant cuvettes interfaced to an IRGA and CF-IRMS via Teflon tubes. The cuvettes were kept in a temperature-controlled cabinet held at the same temperature as the two growth chambers. Each cuvette consisted of an open cylinder (200 mm height, 153 mm diameter) and a top and bottom plate (all made of polyvinylchloride), which could be opened and closed quickly to insert a pot. The bottom plate contained a duct that matched exactly the cross-sectional area of the pot. A similar system was used to seal the bottom of the pot. Rubber seals and vacuum grease ascertained that cuvettes were air tight. Air with known constant $\delta^{13}C$ (−5‰) and concentration of CO_2 (223 μL L^{-1}) was supplied to cuvettes at a rate of 0.75 L min^{-1} after passage of a humidifier. Air flow was controlled by mass flow controllers. Each cuvette had two outlets: one in the shoot section on the opposite side of the inlet, and the other at the bottom of the pot that enclosed the root compartment. Air in the shoot compartment was ventilated by a fan. Part of the air stream feeding the shoot compartment (0.25 L min^{-1}) was drawn through the root compartment with a gas-tight Teflon-lined peristaltic membrane pump. The air was then dried and the flow to a multiway valve block (sample air selector [SAS]) was controlled by a mass flow controller. The remaining air from the shoot compartment was directly conveyed to the SAS. A reference air line (0.9 L min^{-1}) was also connected to the SAS. The SAS sequentially sampled the reference air line and the eight sample air lines and fed the air to the IRGA and CF-IRMS as described by Schnyder et al. (2003).

Prior to measurements, just after removal from the growth chambers, the pots were rinsed with demineralized water, which was previously aerated with CO_2-free air for 1 d. Plants were then enclosed in the respiration cuvettes and the cuvettes flushed with CO_2-free air. After excess water had drained off the bottom section of the cuvette, all measuring air lines were installed and air flow rates were adjusted, as described above. These procedures aimed at removing all extraneous air from shoot and root compartments as quickly as possible.

A full measurement cycle of all four cuvettes was completed in approximately 45 min and included three replicate measurements of $\delta^{13}C$ and concentration of CO_2 in the air exiting the shoot and root compartment of each cuvette plus one reference air measurement. Dark respiration of shoot and root was recorded for about 5 h, thus yielding six full measurements for each plant (compare with Fig. 5). First reliable measurements of the rates and $\delta^{13}C$ of shoot respiration were obtained approximately 30 min after removing plants from the stands, but it took up to 1.5 h to purge the root system free of all extraneous CO_2 (compare with Lötscher et al., 2004). Therefore, it can be ruled out that photorespiratory CO_2 release has contributed to the measured isotopic signal, since the time to purge the cuvettes previous to measurements was much longer than the duration of the (photorespiratory) postillumination burst. Each $\delta^{13}C$ sample was measured against a working gas standard, which was previously calibrated against a VPDB-gauged laboratory CO_2 standard. The SD of repeated single measurements was 0.10‰ for $\delta^{13}C$ and 0.34 μL L^{-1} for the concentration of CO_2 on average of all measurements. The respiration rate of roots decreased slightly (approximately 6%) during the 5-h measurement period, while that of shoots was constant. Average rates were used to calculate specific respiration rates on a carbon basis.

Plant Harvest and Elemental Analysis

Immediately after the termination of respiration measurements, plants were removed from the pots, washed free of sand, dissected into shoot and root, weighed, frozen in liquid nitrogen, and stored at −30°C. All samples were freeze dried for 72 h, weighed again, and ground to flour mesh quality in a ball mill. Aliquots of 0.75 ± 0.05 mg of each sample were weighed into tin cups (IVA Analysentechnik) and combusted in an elemental analyzer (Carlo Erba NA 1110; Carlo Erba Instruments), interfaced to the CF-IRMS, to determine carbon and nitrogen contents.

Analysis of Water-Soluble Carbohydrates

Water-soluble carbohydrates were extracted and quantified as described by Schnyder and de Visser (1999).

Data Analysis

The proportion of carbon in shoot- and root-respired CO_2 that was assimilated before (unlabeled) and during labeling, $f_{unlabeled\text{-}C}$ and $f_{labeled\text{-}C}$ (where $f_{labeled\text{-}C} = 1 - f_{unlabeled\text{-}C}$), was calculated as by Schnyder and de Visser (1999):

$$f_{unlabeled\text{-}C} = (\delta^{13}C_S - \delta^{13}C_{new})/(\delta^{13}C_{old} - \delta^{13}C_{new}) \quad (1)$$

where $\delta^{13}C_S$, $\delta^{13}C_{old}$, and $\delta^{13}C_{new}$ are the $\delta^{13}C$ of respiratory CO_2 produced by the labeled sample plant and by nonlabeled plants growing continuously in

the chamber of origin (old) or in the labeling chamber (new). $\delta^{13}C_S$, $\delta^{13}C_{old}$, and $\delta^{13}C_{new}$ of shoots were obtained as:

$$\delta^{13}C_X = (\delta^{13}C_{in}\,F_{in} - \delta^{13}C_{out}\,F_{out})/(F_{in} - F_{out}) \quad (2)$$

where X stands for sample, new, or old (as appropriate) and $\delta^{13}C_{in}$, $\delta^{13}C_{out}$, F_{in}, and F_{out} are the isotopic signatures and the flow rates of the CO_2 entering and leaving the shoot cuvette. Calculations for the root compartment were done in the same way in considering that the concentration and $\delta^{13}C$ of the CO_2 entering the root compartment was equal to that in the shoot compartment (compare with Klumpp et al., 2005).

The $\delta^{13}C$ of shoot-respired CO_2 of individual control plants as well as that of labeled plants did not change during the 5 h of respiration measurements ($P > 0.05$). From 1.5 h after transfer, the $\delta^{13}C$ of root respiration was also stable (Fig. 5). Barbour et al. (2007) observed rapid and pronounced changes in $\delta^{13}C$ of respired CO_2 during the first few minutes following light-to-dark transition in *Ricinus communis*. We did not observe such an effect, probably because our first measurements started 30 min after removal from the chamber. Thus, $\delta^{13}C$ of respiratory CO_2 of the shoot or root of one plant was taken as the mean of all measurements of that plant. This was true for all measurements, except for shoots labeled for only 1 h: in these, $f_{unlabeled\text{-}C}$ increased markedly during the measurement (Fig. 5), suggesting depletion of a rapidly labeled carbon pool. In that case, regression analysis was applied and $f_{unlabeled\text{-}C}$ was taken as the *y* intercept of the linear regression of $f_{unlabeled\text{-}C}$ (y) versus time after removal from the growth chamber (x; Fig. 5). This procedure ensured that $f_{unlabeled\text{-}C}$ in shoot- and root-respired CO_2 of each plant referred to the same time in darkness and thus provided the basic reference points for the estimation of pool properties.

Carbon isotope discrimination, $\Delta^{13}C$ [defined as $\Delta^{13}C = (\delta^{13}C_{CO2} - \delta^{13}C_{respiratory\ CO2})/(1 + \delta^{13}C_{respiratory\ CO2})$], was determined for nonlabeled plants from both chambers. Chambers did not differ ($P > 0.05$), as would be expected from the fact that growth conditions were the same. However, there was a difference in $\Delta^{13}C$ of shoots and roots (23.2‰ ± 1.0 SD versus 25.8‰ ± 0.7 SD), consistent with the observations of Klumpp et al. (2005). This effect was accounted for in the labeling data evaluation using shoot- and root-specific $\delta^{13}C_{new}$ and $\delta^{13}C_{old}$ values in Equation 1 (see also Schnyder and de Visser, 1999).

Refixation of respiratory CO_2 was considered unimportant in this work. Principally, there are two aspects of refixation that are potentially relevant: one relates to refixation of respiratory CO_2 that has been released into the chamber atmosphere, the other concerns (internal) refixation within the photosynthetic tissue. Refixation of respired CO_2 from the chamber atmosphere was insignificant in this open, rapidly turned-over system, in which the rate of CO_2 supply to the chambers exceeded the stand CO_2 exchange rate by a factor of 9. The carbon isotope composition of CO_2 in the chamber air was measured nearly continuously, and these measurements were taken as the actual source CO_2 isotope composition. Moreover, the small number of labeling plants present in a chamber at any moment had no measurable effect on the isotopic composition of CO_2 in chamber air. Internal refixation was estimated using knowledge of ^{13}C discrimination in shoot biomass, assumptions about the fractional contribution of leaf respiration to stand respiration, and the ratio of respiration to photosynthesis. With a ^{13}C discrimination of 23.0‰, the ratio of leaf internal to atmospheric CO_2 concentration was near 0.82 (Farquhar et al., 1989); thus, the probability for refixation of leaf-respired CO_2 was approximately 18%. Assuming that leaf-respired carbon accounted for about one-third of plant respiration and that total plant respiration in light was one-third of the photosynthetic flux, the contribution of refixation to total photosynthetic CO_2 fixation was approximately 1.6% ($0.18 \times 0.3 \times 0.3 = 0.016 = 1.6\%$). This effect was considered insignificant.

Compartmental Modeling of Tracer Time Course in Respired CO_2

The model shown in Figure 3 was described mathematically assuming that the system was in steady state, an assumption supported by constant specific growth and respiration rates of shoots and roots. Estimated turnover rates and half-lives assume first-order kinetics.

The fraction of tracer in each compartment with respect to time was given by:

$$f_{unlabeled\text{-}C\text{-}Q1} = (Q_1 \times f_{unlabeled\text{-}C\text{-}Q1} + F_{In} \times f_{labeled\text{-}C} - F_{10} \times f_{unlabeled\text{-}C\text{-}Q1} - F_{12} \times f_{unlabeled\text{-}C\text{-}Q1})/Q_1 \quad (3a)$$

$$f_{unlabeled\text{-}C\text{-}Q2} = (Q_2 \times f_{unlabeled\text{-}C\text{-}Q2} + F_{12} \times f_{unlabeled\text{-}C\text{-}Q1} + F_{32} \times f_{unlabeled\text{-}C\text{-}Q3} - F_{23} \times f_{unlabeled\text{-}C\text{-}Q2} - F_{20} \times f_{unlabeled\text{-}C\text{-}Q2})/Q_2 \quad (3b)$$

$$f_{unlabeled\text{-}C\text{-}Q3} = (Q_3 \times f_{unlabeled\text{-}C\text{-}Q3} + F_{23} \times f_{unlabeled\text{-}C\text{-}Q2} - F_{32} \times f_{unlabeled\text{-}C\text{-}Q3})/Q_3 \quad (3c)$$

$$f_{unlabeled\text{-}C} = (F_{10} \times f_{unlabeled\text{-}C\text{-}Q1} + F_{20} \times f_{unlabeled\text{-}C\text{-}Q2})/(F_{10} + F_{20}) \quad (3d)$$

where Q_1, Q_2, and Q_3 are the pool sizes and F_{In} is the flux of photosynthetically assimilated carbon (tracer) that enters the respiratory system. Since the system is in steady state and F_{In} equals the specific respiration rate, $F_{In} = F_{Out}$, $F_{Out} = F_{10} + F_{20}$ (Fig. 3), $F_{12} = F_{20}$, and $F_{23} = F_{32}$. Indices refer to donor and receptor pools, respectively. Index 0 represents the environment. The fraction of unlabeled carbon in shoot- or root-respired CO_2 is $f_{unlabeled\text{-}C}$. This is the measured parameter against which the model prediction is compared. $f_{unlabeled\text{-}C\text{-}Qi}$ is the fraction of unlabeled carbon in the pool Q_i, and $f_{labeled\text{-}C}$ is the constant fraction of fully labeled carbon entering the system after the start of labeling.

In order to fit the initial part of the tracer time course observed in root respiration, delay 2 was inserted between the beginning of labeling and the start of tracer incorporation in Q_1. In other words, tracer entered Q_1 in the root model a little later than in the shoot model, which would account for phloem transport time from shoot to root. Delay 2 was not necessary to simulate the tracer time course observed in shoot respirations.

To model the stable degree of labeling in the first hours (Fig. 2, insets), delay 1 between tracer acquisition in pool Q_2 and its efflux in F_{20} (Fig. 3) was required in both shoot and root simulations. Mathematically, $f_{unlabeled\text{-}C\text{-}Q2}$ in Equation 3d was forced to lag temporally behind $f_{unlabeled\text{-}C\text{-}Q2}$ in Equations 3b and 3c for the numerical value of delay 1. Since delay 1 operated only on the release side of Q_2 (i.e. F_{20}), it had no effect on the estimation of the half-lives of Q_2 and Q_3. Considering the steady state of the system, it is important to note that delay 1 and delay 2 only apply to tracer content in respired CO_2 and not to the rate of respiration itself.

These equations were implemented in a custom-made program using the free software R (R Development Core Team, 2007). Initial values for pool sizes, fluxes between pools, and delays were inserted, and the set of numerical equations (Eqs. 3a–3d) was solved. In that way, a tracer time course across the entire labeling period (600 h) was generated. The goodness of the fit was expressed as the RMSE:

$$RMSE = \sqrt{\frac{\sum_{i=1}^{n}\left(x\left(t_i\right) - X\left(t_i\right)\right)^2}{n}} \quad (4)$$

with *x* and *X* the observed and model-predicted $f_{unlabeled\text{-}C}$ at labeling time *i*, and *n* the number of labeling times.

This procedure was followed many times by stepwise and systematic variation of pool sizes, fluxes, and delays to identify the combination of values yielding the minimum RMSE (Table I; Fig. 4).

Optimized pool sizes and fluxes served to calculate the half-life ($t_{1/2}$) of a pool of size Q_i:

$$t_{1/2}(Q_i) = \ln(2)/(F_i/Q_i) \quad (5)$$

with F_i the sum of all fluxes leaving the pool Q_i.

Based upon optimized fluxes, the contribution of a pool Q_i (C_{Qi}) to respiratory carbon release was derived, which is defined here as the probability of tracer moving in a certain flux of the respiratory system (compare with Fig. 3):

$$C_{Q1} = F_{10}/(F_{10} + F_{12}) \quad (6a)$$

$$C_{Q2} = (1 - F_{10}/(F_{10} + F_{12})) \times F_{20}/(F_{20} + F_{23}) \quad (6b)$$

$$C_{Q3} = (1 - F_{10}/(F_{10} + F_{12})) \times F_{23}/(F_{20} + F_{23}) \quad (6c)$$

$$C_{Q1} + C_{Q2} + C_{Q3} = 0.95$$

C_{Q1} is thus the probability that tracer enters the system and leaves it in F_{10} without visiting any other pool. C_{Q2} implies that tracer enters Q_2 via Q_1 and is

respired in F_{20} without moving through Q_3. C_{Q3} is the probability of tracer cycling through the storage pool at least once.

Validity of Model Assumptions

As is the general case for compartmental analyses (Farrar, 1990; Lattanzi et al., 2005), ours was based on the assumptions that (1) the system is in a steady state, (2) fluxes obey first-order kinetics, and (3) pools are homogeneous and well mixed (Farrar, 1990; Lattanzi et al., 2005). Assumption 1 was well satisfied in the experiment: specific growth and respiration rates of shoots and roots were constant (see "Results" and "Discussion"). Also, the carbon to nitrogen ratio of biomass (24:1) did not change ($P > 0.05$; data not shown). Growing plants in continuous light ensured that short-term changes of pool sizes and fluxes (which are common to plants growing in day/night cycles) did not occur. Assumption 2 is probably false in a strict sense, but its practical validity seems supported (see Farrar, 1990, for discussion).

Assumption 3 is perhaps the most drastic simplification in the model. Probably, the different pools are not truly homogeneous but may constitute several biochemical compounds located in different spatial compartments, such as protein and fructan pools in different leaves. However, further compartmentalization did not improve goodness of fit, indicating that the kinetic properties of the components of a pool were similar. The observed lags for tracer arrival in the root and respiratory carbon release from Q_2 represent exemptions from the well-mixing assumption, which were explicitly accounted for by inserting (and optimizing) appropriate delays.

Tracer studies normally assume that isotopic discrimination in pool exchange processes can be neglected. In our study, any effects of carbon isotope fractionation during photosynthesis, transport, and metabolism on carbon isotope composition of respired CO_2 were accounted for in the evaluation of labeling data by assessing (and correcting for) isotopic discrimination in unlabeled plants (de Visser et al., 1997).

ACKNOWLEDGMENTS

The members of the Lehrstuhl für Grünlandlehre (Technische Universität Munich) are thanked for helpful discussions, particularly Karl Auerswald and Ulrike Gamnitzer. Expert technical assistance was provided by Wolfgang Feneis during the experimental period, by Anja Schmidt in carbohydrate analyses, and by Max Wittmer in the writing of the R program. C.A.L. thanks Union Brunnhofen for continuous support.

Received July 30, 2008; accepted August 13, 2008; published August 20, 2008.

LITERATURE CITED

Allard G, Nelson CJ (1991) Photosynthate partitioning in basal zones of tall fescue leaf blades. Plant Physiol **95:** 663–668

Amthor JS (1989) Respiration and Crop Productivity. Springer Verlag, New York

ap Rees T (1980) Assessment of the contributions of metabolic pathways to plant respiration. *In* DD Davies, ed, The Biochemistry of Plants: A Comprehensive Treatise, Vol 2. Academic Press, San Diego, pp 1–29

Atkins GL (1969) Multicompartment Models in Biological Systems. Methuen, London

Avice JC, Ourry A, Lemaire G, Boucoud J (1996) Nitrogen and carbon flows estimated by ^{15}N and ^{13}C pulse-chase labeling during regrowth of alfalfa. Plant Physiol **112:** 281–290

Barbour MM, McDowell NG, Tcherkez G, Bickford CP, Hanson DT (2007) A new measurement technique reveals rapid post-illumination changes in the carbon isotope composition of leaf-respired CO_2. Plant Cell Environ **30:** 469–482

Bell CJ, Incoll LD (1982) Translocation from the flag leaf of winter wheat in the field. J Exp Bot **33:** 896–909

Borland AM, Farrar JF (1988) Compartmentation and fluxes of carbon in leaf blades and leaf sheaths of *Poa annua* L. and *Poa x jemtlandica* (Almq.) Richt. Plant Cell Environ **11:** 535–543

Bürkle L, Hibberd JM, Quick WP, Kühn C, Hirner B, Frommer WB (1998) The H^+-sucrose cotransporter NtSUT1 is essential for sugar export from tobacco leaves. Plant Physiol **118:** 59–68

Calvin M, Bassham JA (1962) The Photosynthesis of Carbon Compounds. WA Benjamin, New York

Davidson JL, Milthorpe FL (1966a) Leaf growth in *Dactylis glomerata* following defoliation. Ann Bot (Lond) **30:** 173–184

Davidson JL, Milthorpe FL (1966b) The effect of defoliation on the carbon balance in *Dactylis glomerata*. Ann Bot (Lond) **30:** 185–198

de Visser R, Vianden H, Schnyder H (1997) Kinetics and relative significance of remobilized and current C and N incorporation in leaf and root growth zones of *Lolium perenne* after defoliation: assessment by ^{13}C and ^{15}N steady-state labelling. Plant Cell Environ **20:** 37–46

Dewar RC, Medlyn BE, McMurtrie RE (1998) A mechanistic analysis of light and carbon use efficiencies. Plant Cell Environ **21:** 573–588

Dilkes NB, Jones DL, Farrar J (2004) Temporal dynamics of carbon partitioning and rhizodeposition in wheat. Plant Physiol **134:** 706–715

Dungey NO, Davies DD (1982) Protein turnover in the attached leaves of non-stressed and stressed barley seedlings. Planta **154:** 435–440

Farquhar GD, Ehleringer JR, Hubick KT (1989) Carbon isotope discrimination and photosynthesis. Annu Rev Plant Physiol Plant Mol Biol **40:** 503–537

Farrar JF (1980) Allocation of carbon to growth, storage and respiration in the vegetative barley plant. Plant Cell Environ **3:** 97–105

Farrar JF (1989) Fluxes and turnover of sucrose and fructans in healthy and diseased plants. J Plant Physiol **134:** 137–140

Farrar JF (1990) The carbon balance of fast-growing and slow-growing species. *In* H Lambers, ML Cambridge, H Konings, TL Pons, eds, Causes and Consequences of Variation in Growth Rate and Productivity of Higher Plants. SPB Academic Publishing, The Hague, The Netherlands, pp 241–256

Farrar SC, Farrar JF (1986) Compartmentation and fluxes of sucrose in intact leaf blades of barley. New Phytol **103:** 645–657

Geiger DR, Ploeger BJ, Fox TC, Fondy BR (1983) Sources of sucrose translocated from illuminated sugar beet source leaves. Plant Physiol **72:** 964–970

Geiger DR, Saunders MA, Cataldo DA (1969) Translocation and accumulation of translocate in the sugar beet petiole. Plant Physiol **44:** 1657–1665

Geiger DR, Swanson CA (1965) Evaluation of selected parameters in a sugar beet translocation system. Plant Physiol **40:** 942–947

Heber U, Willenbrink J (1964) Sites of synthesis and transport of photosynthetic products within the leaf cell. Biochim Biophys Acta **82:** 313–324

Heldt HW (2005) Plant Biochemistry. Elsevier Academic Press, San Diego

Imsande J, Touraine B (1994) N demand and the regulation of nitrate uptake. Plant Physiol **105:** 3–7

Jacquez JA (1996) Compartmental Analysis in Biology and Medicine, Ed 3. Biomedware, Ann Arbor, MI

Klumpp K, Schäufele R, Lötscher M, Lattanzi FA, Feneis W, Schnyder H (2005) C-isotope composition of CO_2 respired by shoots and roots: fractionation during dark respiration? Plant Cell Environ **28:** 241–250

Kouchi H, Akao S, Yoneyama T (1986) Respiratory utilization of ^{13}C-labelled photosynthate in nodulated root systems of soybean plants. J Exp Bot **37:** 985–993

Kouchi H, Nakaji K, Yoneyama T, Ishizuka J (1985) Dynamics of carbon photosynthetically assimilated in nodulated soya bean plants under steady-state conditions. 3. Time-course study on ^{13}C incorporation into soluble metabolites and respiratory evolution of $^{13}CO_2$ from roots and nodules. Ann Bot (Lond) **56:** 333–346

Lattanzi FA, Schnyder H, Thornton B (2005) The sources of carbon and nitrogen supplying leaf growth: assessment of the role of stores with compartmental models. Plant Physiol **137:** 383–395

Lea PJ, Ireland RJ (1999) Nitrogen metabolism in higher plants. *In* BK Singh, ed, Plant Amino Acids. Marcel Dekker, New York, pp 1–47

Leport L, Kandlbinder A, Baur B, Kaiser WM (1996) Diurnal modulation of phosphoenolpyruvate carboxylation in pea leaves and roots as related to tissue malate concentrations and to the nitrogen source. Planta **198:** 495–501

Lötscher M, Gayler S (2005) Contribution of current photosynthates to root respiration of non-nodulated *Medicago sativa*: effects of light and nitrogen supply. Plant Biol **7:** 601–610

Lötscher M, Klumpp K, Schnyder H (2004) Growth and maintenance respiration for individual plants in hierarchically structured canopies of *Medicago sativa* and *Helianthus annuus*: the contribution of current and old assimilates. New Phytol **164:** 305–316

Moorby J, Jarman PD (1975) The use of compartmental analysis in the study of the movement of carbon through leaves. Planta **122:** 155–168

Nogués S, Tcherkez G, Cornic G, Ghashghaie J (2004) Respiratory carbon metabolism following illumination in intact French bean leaves using $^{13}C/^{12}C$ isotope labeling. Plant Physiol **136:** 3245–3254

Plaxton WC, Podestá FE (2006) The functional organization and control of plant respiration. Crit Rev Plant Sci **25:** 159–198

Pollock CJ, Cairns AJ (1991) Fructan metabolism in grasses and cereals. Annu Rev Plant Physiol Plant Mol Biol **42:** 77–101

Prosser PJ, Farrar JF (1981) A compartmental model of carbon allocation in the vegetative barley plant. Plant Cell Environ **4:** 303–307

R Development Core Team (2007) R: A Language and Environment for Statistical Computing. R Foundation for Statistical Computing, Vienna. http://www.R-project.org (December 16, 2007)

Ratcliffe RG, Shachar-Hill Y (2006) Measuring multiple fluxes through plant metabolic networks. Plant J **45:** 490–511

Rescigno A (2001) The rise and fall of compartmental analysis. Pharmacol Res **44:** 337–342

Rocher JP, Prioul JL (1987) Compartmental analysis of assimilate export in a mature maize leaf. Plant Physiol Biochem **25:** 531–540

Ryle GJA, Cobby JM, Powell CE (1976) Synthetic and maintenance respiratory losses of $^{14}CO_2$ in uniculm barley and maize. Ann Bot (Lond) **40:** 571–586

Schimel DS (1995) Terrestrial ecosystems and the carbon-cycle. Glob Change Biol **1:** 77–91

Schnyder H, de Visser R (1999) Fluxes of reserve-derived and currently assimilated carbon and nitrogen in perennial ryegrass recovering from defoliation: the regrowing tiller and its component functionally distinct zones. Plant Physiol **119:** 1423–1435

Schnyder H, Nelson CJ (1987) Growth rates and carbohydrate fluxes within the elongation zone of tall fescue leaf blades. Plant Physiol **85:** 548–553

Schnyder H, Schäufele R, Lötscher M, Gebbing T (2003) Disentangling CO_2 fluxes: direct measurements of mesocosm-scale natural abundance $^{13}CO_2/^{12}CO_2$ gas exchange, ^{13}C discrimination, and labelling of CO_2 exchange flux components in controlled environments. Plant Cell Environ **26:** 1863–1874

Simpson E, Cooke RJ, Davies DD (1981) Measurement of protein degradation in leaves of *Zea mays* using [^{3}H]acetic anhydride and tritiated water. Plant Physiol **67:** 1214–1219

Smith AM, Stitt M (2007) Coordination of carbon supply and plant growth. Plant Cell Environ **30:** 1126–1149

Stitt M, Müller C, Matt P, Gibon Y, Carillo P, Morcuende R, Scheible WR, Krapp A (2002) Steps towards an integrated view of nitrogen metabolism. J Exp Bot **53:** 959–970

Sullivan JT, Sprague VG (1943) Composition of the roots and stubble of perennial ryegrass following partial defoliation. Plant Physiol **18:** 656–670

Tcherkez G, Nogués S, Bleton J, Cornic G, Badeck F, Ghashghaie J (2003) Metabolic origin of carbon isotope composition of leaf dark-respired CO_2 in French bean. Plant Physiol **131:** 237–244

Trumbore S (2006) Carbon respired by terrestrial ecosystems: recent progress and challenges. Glob Change Biol **11:** 1–13

van Iersel MW (2003) Carbon use efficiency depends on growth respiration, maintenance respiration, and relative growth rate: a case study with lettuce. Plant Cell Environ **26:** 1441–1449

Vijn I, Smeekens S (1999) Fructan: more than a reserve carbohydrate? Plant Physiol **120:** 351–359

Windt CW, Vergeldt FJ, de Jager PA, Van As H (2006) MRI of long-distance water transport: a comparison of the phloem and xylem flow characteristics and dynamics in poplar, castor bean, tomato and tobacco. Plant Cell Environ **29:** 1715–1729

Winzeler M, Dubois D, Nösberger J (1990) Absence of fructan degradation during fructan accumulation in wheat stems. J Plant Physiol **136:** 324–329